

## CHAPTER 24

# A New Type Breaker Forming a Giant Jet and its Decaying Properties

Takashi Yasuda<sup>1</sup>, M.ASCE Hidemi Mutsuda<sup>2</sup>, Atsushi Oya<sup>3</sup>,  
Akihide Tada<sup>4</sup> and Tadashi Fukumoto<sup>4</sup>

### Abstract

Experiments in a wave flume(1m × 2m × 65m) with 16 wave gages and numerical simulations using a fully nonlinear BIM(Boundary Integral Method) in a super-computer(VP2600) are conducted to make clear the characteristics and occurrence condition of a new type breaker. Further, its deformation and wave height decay after breaking are investigated. It is shown that the new type breaker forms a giant jet with the size exceeding three times of the maximum jet size of usual type breakers and therefore is very efficient to wave control because of strong turbulence excited by plunging of the giant jet and the resultant remarkable absorption.

### 1. Introduction

Wave control and shore protection works utilizing artificial reef and submerged breakwater have many advantages over usual coastal structures such as offshore breakwater. However, since most breaking waves caused by the submerged coastal structures are spilling or plunger and they cannot excite sufficiently strong turbulence responsible to the required wave absorption, the problem that the efficiency of wave absorption is insufficient arises from those submerged structures. For that reason, in order to increase the efficiency and develop the artificial reef work to a desirable wave control and shore protection work, it is required to generate a breaker exciting much stronger turbulence and strengthen the absorption due to wave breaking.

However, a good understanding and information of the mechanism for breaker types that are essentially important for the energy absorption are still very limited. Nevertheless, most breaking waves have been supposed to be classified into four breaker types, spilling, plunging, collapsing and surging, based on

---

<sup>1</sup>Prof., Dept. of Civil Eng., Gifu Univ., Yanagido 1-1 Gifu 501-11, Japan

<sup>2</sup>Res. Assoc., ditto

<sup>3</sup>Graduate student, Graduate school of Gifu Univ., ditto

<sup>4</sup>Res. Eng., Tech. Res. Inst., Nishimatsu Construction Co. Ltd., Yamato 242, Japan

the visual observations of periodic waves regarding uniformly sloping bottoms, and accordingly little attention has been given to the possibility of new breaker types.

Cooker et al.(1990) studied the interaction between a solitary wave and a submerged semicircular cylinder, and found that the breaker forms are governed by the extent of the crest exchanges between the incident crest and the 2nd crest excited on the downward side of the cylinder. The results show that the breaker suffering the crest exchange is clearly different from the breaking of nonlinear long waves, in which the higher parts of an incident wave travel faster due to shallow water steepening and finally overturns to eject a jet, and reveals various behaviors and forms dependent on the interaction between the incident crest and the 2nd one.

In order to find out a new type breaker forming a giant jet and being efficient to wave absorption, we have been investigating basically the mechanism and characteristics of the breakers caused by submerged obstacles. As a result, such a breaker forming a giant jet was found to occur when a solitary wave strikes a reef having two steps, referred here to as a double reef. This breaker could be expected applicable to efficient wave control because it excites strong turbulence by plunging of the giant jet. Further, the new type breaker could be generated independently of these kinds of waves and bottom topography, only if the given conditions can be satisfied.

In this study, a solitary wave is made as an incident wave and is allowed to strike reefs having single and two steps with various heights, in order to reduce the number of parameters related to wave breaking as few as possible. Numerical simulations of the overturning of solitary waves on reefs are carried out until the jets ejected from their crests begin to fall, in order to investigate the characteristics of breaking wave profile and jet size and make clear the occurrence condition of the aforementioned new type breaker forming a giant jet. Further, experiments are conducted to verify the generation of the new type breaker in real fluid. At the same time, the accuracy of the simulated results is examined and the properties of wave deformation and wave height decay after breaking is made clear.

## 2. Method and Condition

### 2.1 Computations

Numerical computations using a fully-nonlinear BIM irrotational-flow model (Yasuda et al., 1990) are carried out of the overturning of solitary waves on reefs having single and two steps (Fig .1) until the jet-fall initiation, defined as when the overhanging face beneath the jet becomes just horizontal and the maximum

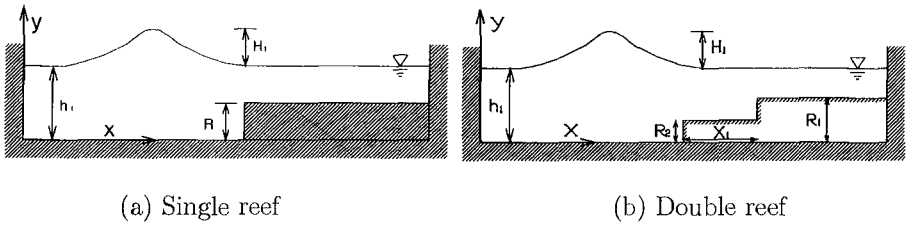


Figure 1: Coordinates and symbols for computations

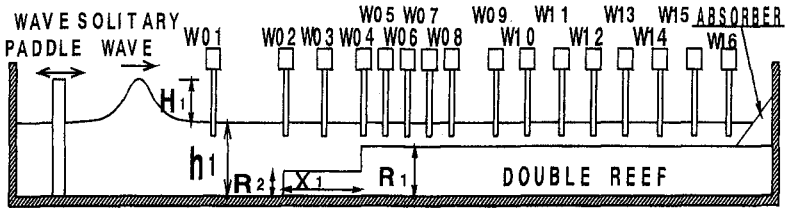


Figure 2: Wave flume and locations of wave gages

gradient angle  $\theta$  of the front face at each time step reaches  $180^\circ$ . Here, while a reef shown in Fig.1(a) is referred to as a single reef, a reef having two steps is referred to as a double reef.

The accuracy of the computations was previously examined by comparing a computed solitary wave with its exact solution and further verifying the validity of the computed surface profiles and water particle velocities at the breaking against carefully controlled experiments (Yasuda et al., 1992, 1993).

As an initial condition, a solitary wave represented by the exact solution (Tanaka, 1986) of a fully-nonlinear irrotational flow theory is given over the flat bed of the left-hand side of each reef as illustrated in Fig.1, and is assumed to propagate toward the reef. The numerical computations were undertaken under the condition that the error for energy conservation law is always less than 1%.

## 2.2 Experiments

Experiments were conducted in a 65m long, 1m wide and 2m high wave flume with a side window. Solitary waves with incident wave heights of 9.15cm  $\sim$  16.90cm were generated using a computer-controlled piston wave maker. The still water depth  $h_1$  was fixed to 31.0cm. Reef models made of steel plate were built on the plane bottom, 30.0m distant from the wave paddle. The height  $R$  of a single reef is 26.3cm, and the lower crown height  $R_2$  and the upper one  $R_1$  of a double reef are 13.1cm and 26.3cm respectively. A relative distance  $X_1$  between

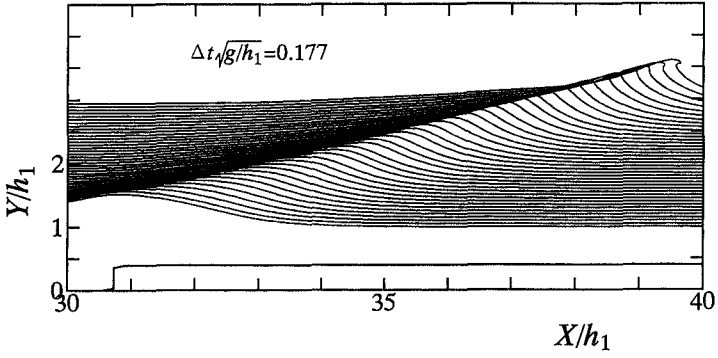
the 1st step and 2nd one of a double reef was changed from 0.0cm to 250.0cm. The case of  $X_1 = 0.0\text{cm}$  corresponds to the single reef ( $R_2 = 0.0\text{cm}$ ).

16 capacitance wave gages were installed to measure the temporal water surface elevation at each location shown in Fig.2. The gage W01 was placed in front of the reef to measure the incident wave profile and height. A high-speed video camera(unic, HSV-400) with a speed of 200 frames per second was used simultaneously to record the profile and size of the overturning jet.

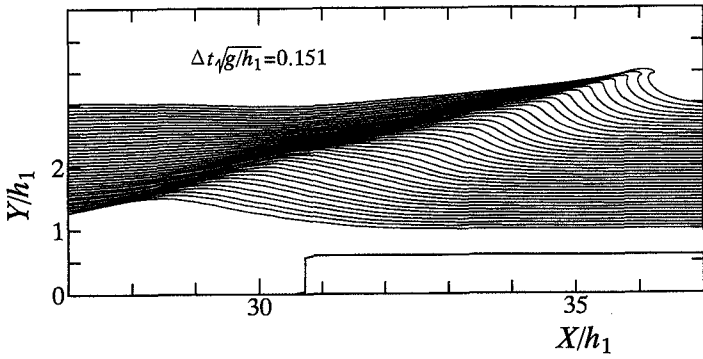
### 3. Wave Breaking on a Single Reef

Time evolutions of spatial surface profiles of a solitary wave incident to single reefs with  $R/h_1 = 0.4, 0.6$  and  $0.9$  are introduced here. The evolutions up to jet-fall initiation are illustrated in Fig.3, in which  $\Delta t \sqrt{g/h_1}$  indicates the non-dimensionalized time increment of each evolution. The incident wave shown in Fig.3(a) does not accompany the 2nd crest and steepens to eject a small jet from the crest point at the location of  $X/h_1 \approx 8$ . This breaker therefore could be regarded as a spiller type. In the case of a single reef with a relative crown height of  $R/h_1 = 0.6$ , the breaker could be regarded as a plunger type because it had a larger jet than that of a spiller type. Further, the 2nd crest is generated from the front face and grows to eject a jet from the crest at the position of  $X/h_1 \approx 4$  through the crest exchange with the incident crest, while the incident crest vanishes after having finished the crest exchange. Although this crest exchange is apparently similar with the soliton-soliton overtaking interaction as pointed out by Cooker et al.(1990), more information about it needs to be known. Furthermore, in the case of a single reef with  $R/h_1 = 0.9$ , the 2nd crest is generated far before the incident crest approaches the step, and then promptly ejects the jet at the position of  $X/h_1 \approx 2$  during the crest exchange, while the incident crest keeps a height exceeding the 2nd crest. As a result, the jet seems to be ejected from lower part of the front face of the incident wave and therefore is regarded as a collapsing breaker.

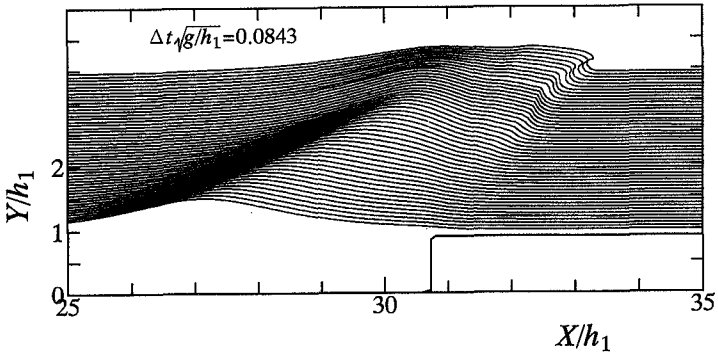
In order to examine the relation of the profile and size of the jet to the relative crown height  $R/h_1$ , comparisons of surface profiles around the jet are made for the solitary waves incident to single reefs with  $R/h_1 = 0.25 \sim 0.90$ , and their profiles at the breaking limit, defined as an instant that the forward face first becomes vertical and the maximum gradient angle  $\theta$  just reaches  $90^\circ$ , and the jet-fall initiation are shown in Fig.4. It is found from the surface profiles at  $\theta = 90^\circ$  that their horizontal asymmetries correspond well to the crown heights of reefs. It is also noticed that the vertical location of the jet tip at  $\theta = 180^\circ$  becomes lower with the increasing of the reef height. However, the size of the jet seems to grow with the increase of the reef height while the profile of the jet keeps similarity.



(a)  $R/h_1 = 0.4$

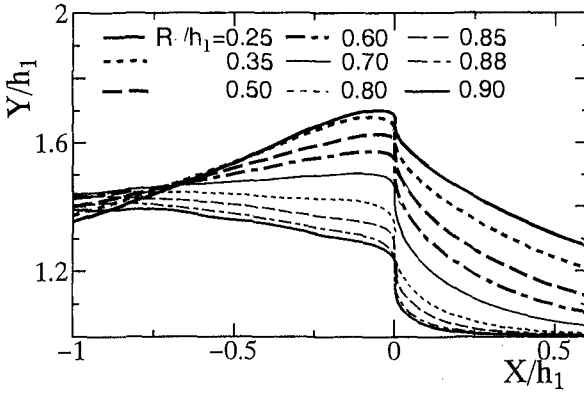


(b)  $R/h_1 = 0.6$

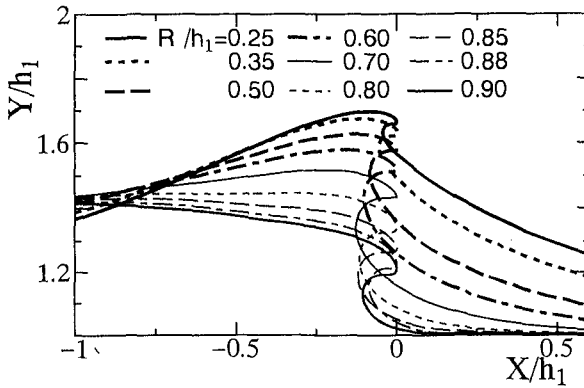


(c)  $R/h_1 = 0.9$

Figure 3: Propagation process up to overturning of a solitary wave with  $H_1/h_1 = 0.5$  on single reefs with  $R/h_1 = 0.4, 0.6$  and  $0.9$



(a) Breaking limit( $\theta = 90^\circ$  )



(b) Jet-fall initiation( $\theta = 180^\circ$  )

Figure 4: Comparisons of wave profiles at the breaking limit( $\theta = 90^\circ$  ) and jet-fall initiation( $\theta = 180^\circ$  )

Further, in order to examine a quantitative relationship between the jet size and the reef height, we first define the horizontal jet length  $\gamma$  and the jet height  $\eta_J$  at the jet-fall initiation ( $\theta = 180^\circ$  ), as illustrated in Fig.5, and further show the correlation under the incident wave heights of  $H_1/h_1 = 0.4, 0.5$  and  $0.6$  between the relative jet size  $S = \gamma\eta_J/H_1^2$  and the relative reef height  $R/h_1$  in Fig.6. The relative jet size  $S$  is found not to grow monotonically with the increase of the reef height but to have the maximum value dependent on the value of  $H_1/h_1$ . This shows that the breaking waves accompanying the jet of which size exceeds  $0.06$  under the incident wave heights of  $H_1/h_1 = 0.4, 0.5$  and  $0.6$  never occur on single reefs even if the reef height  $R$  increases up to the water depth  $h_1$ .

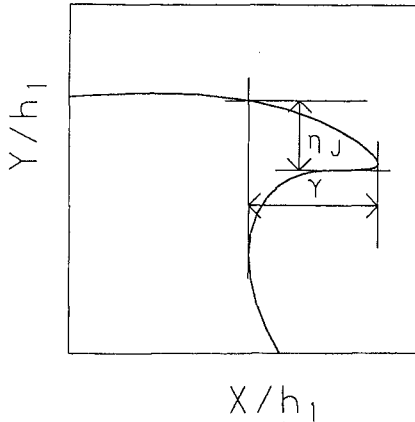


Figure 5: Definition diagram of the horizontal jet length  $\gamma$  and the jet height  $\eta_J$  at the jet-fall initiation

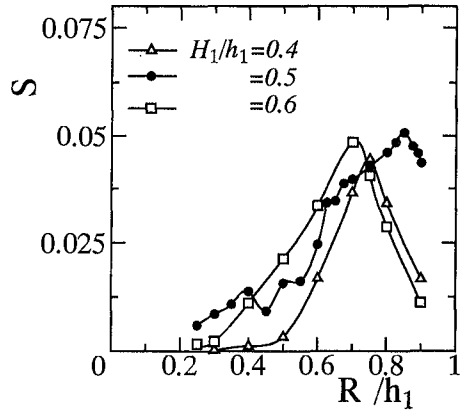


Figure 6: Relations of the jet size parameter  $S$  to the ratio of incident wave height to water depth  $H_1/h_1$  and the relative crown height of the single reef  $R/h_1$

#### 4. New Type Breaker on a Double Reef

The surface profiles of a new type breaker on a double reef are shown in Photo 1. It is clearly found from the profiles that the new type breaker is characterized by the height of the location ejecting a jet, which is not the crest point and lower-half part of the wave, but is the upper part of the front face, and by the overturning jet form having a triangular crown. Such a breaker can never be categorized by the usual four types defined by Galvin(1968), and therefore, should be recognized as a new type breaker out of doubt. The snapshots further demonstrate the generation of the 2nd crest from the forward face and the formation of a giant jet excited by the coupling of the near-breaking incident crest and the 2nd one. Thus, the new type breaker is characterized by the formation of the giant jet having a triangular crown through the composition of both the crests and therefore is referred to as a composite breaker.

Figure 7 shows time evolutions of the numerically computed spatial surface profile of a solitary wave with  $H_1/h_1 = 0.5$  incident to a double reef with  $R_1/h_1 = 0.8$ ,  $R_2/h_1 = 0.4$  and  $X_1/h_1 = 6.5$ , in which the 2nd step is located near the point of breaking of the incident wave caused by the 1st step. The features of the composite breaker demonstrated by the snapshots are clearly found in the computed results. The 2nd crest generated from the forward face grows fast to eject the jet through the crest exchange with the near-breaking incident crest, as found from the distance between the 2nd step and the position of the ejection

of the jet.

The incident crest suffers the decaying effect due to the crest exchange with 2nd crest and the shoaling effect due to the 2nd step, and consequently, its steep profile is strongly held under the nonlinear interaction. This strongly held triangular crest joins up with the 2nd crest to form a giant jet. Thus, the composite breaker is supposed to be generated by the composition of the triangular incident crest strongly held by the reciprocal effects of decaying and shoaling and the overturning 2nd crest.

Figure 8 indicates comparisons of the breaking wave profiles shown in Photo 1 between the results processing from the images captured with the high-speed video camera and the computed ones shown in Fig.7. The computed profiles agree very well with the experimental ones, although the numerical computation was performed under the assumption of irrotational flow in an incompressible and inviscid fluid. The results obtained assure again that the present BIM is applicable for investigating the breaking wave problem without performing any experimental work, and further, verify that a new type breaker forming a giant jet, that is, a composite breaker can be generated on a double reef.



Photo 1 : Snapshots of the composite breaker from the generation of the 2nd crest to the jet-fall initiation

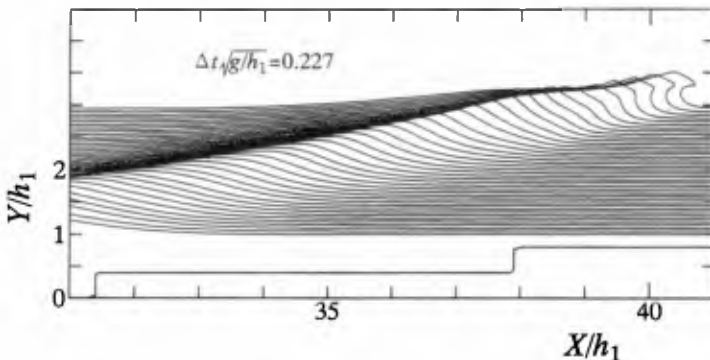


Figure 7: Propagation process of a solitary wave leading to composite breaker on a double reef with  $R_1/h_1 = 0.8$ ,  $R_2/h_1 = 0.4$  and  $X_1/h_1 = 6.5$ .



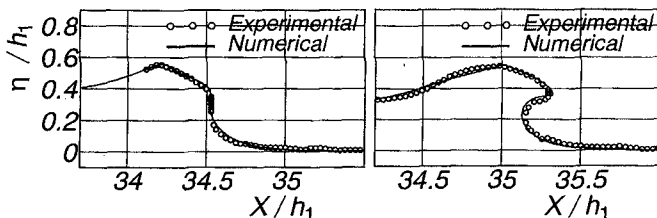
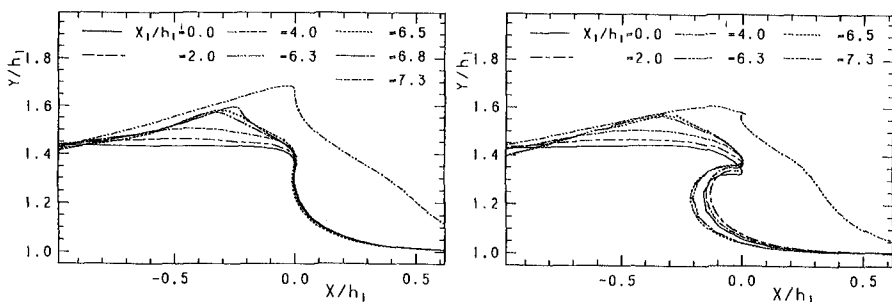


Figure 8: Comparisons of spatial surface profiles at breaking and jet-fall initiations between the results processed from images captured with a high-speed video camera and the numerically computed ones



(a) Breaking limit( $\theta = 90^\circ$  )      (b) Jet-fall initiation( $\theta = 180^\circ$  )

Figure 9: Relations of wave profiles at the breaking and jet-fall initiations to the relative step distance  $X_1/h_1$  of the double reef

In order to examine the relation of the profile and size of the jet to the relative step distance  $X_1/h_1$ , comparisons of surface profiles around the jet at the breaking and jet-fall initiations are made for a solitary wave with  $H_1/h_1 = 0.5$  incident to the double reefs with  $R_1/h_1 = 0.8$ ,  $R_2/h_1 = 0.4$  and  $X_1/h_1 = 0.0 \sim 7.3$  and their results are shown in Fig.9. The incident crest turns to reveal triangular form and its height exceeds that of the breaker on a single reef( $X_1/h_1 = 0.0$ ), as the relative step distance  $X_1/h_1$  increases. However, when the value of  $X_1/h_1$  exceeds about 7.0, a small jet is ejected from the incident crest before the incident crest gets to be combined with the 2nd one and then a giant jet is formed. For that reason, the jet size remarkably decreases in  $X_1/h_1 = 7.3$  as shown in Fig.9(b).

Further, in order to make clear quantitatively the relation of the jet size  $S$  of breakers on double reefs to the relative 1st step height  $R_2/h_1$  and step distance  $X_1/h_1$ , we show the relations under the conditions of  $H_1/h_1 = 0.5$ ,  $R_1/h_1 = 0.8$ ,  $R_2/h_1 = 0.3 \sim 0.6$  and  $X_1/h_1 = 0.0 \sim 10.0$  in Fig.10. While the jet sizes of usual

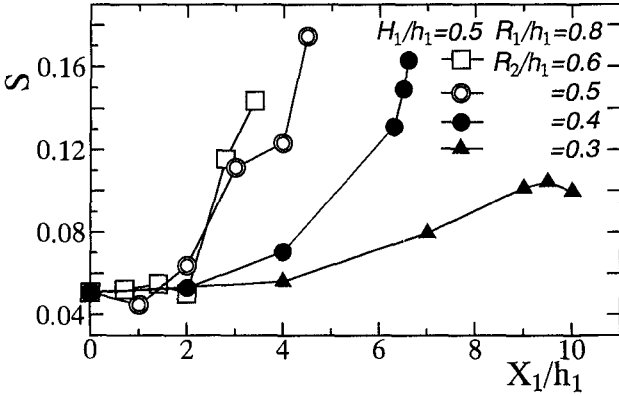


Figure 10: Relations of the jet size parameter  $S$  of the breaking wave with an incident wave height  $H_1/h_1 = 0.5$  caused by double reefs with  $R_1/h_1 = 0.8$ ,  $R_2/h_1 = 0.3 \sim 0.6$  and  $X_1/h_1 = 0.0 \sim 10.0$ .

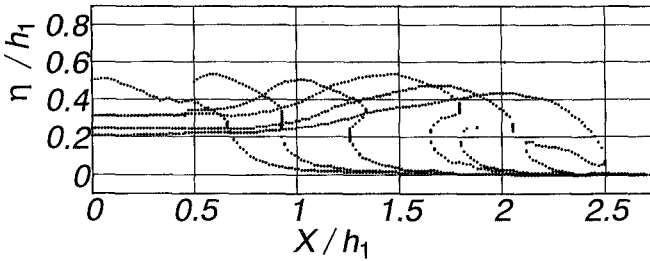


Figure 11: Overturning process of a composite breaker obtained by image processing

type breakers generated on a single reef can never exceed the maximum value as previously shown in Fig.6, the jet size of the composite breaker generated on a double reef grows with an increase in  $X_1/h_1$  and at last exceeds 0.16, that is, three times of the maximum jet size  $S \doteq 0.05$  of usual type breakers introduced in Fig.6 when the location of the 2nd step is close to the breaking point of the incident wave.

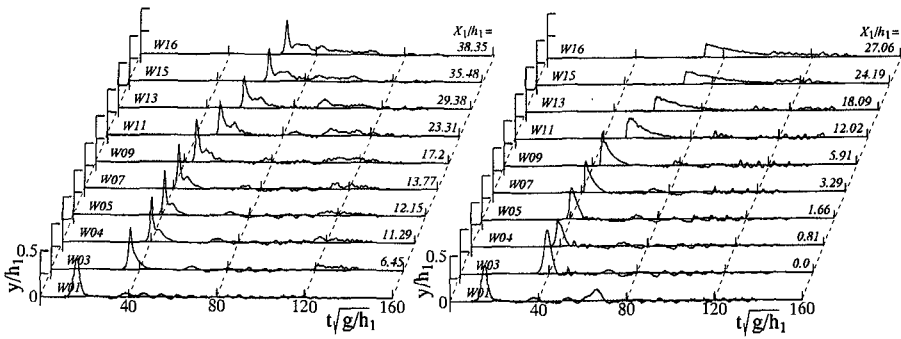
### 5. Deformation and Decay After Breaking

Deformation of wave profile and decay of wave height after breaking are investigated and then their characteristics for composite breaker are made clear, by analyzing the data of water surface elevations at 16 measuring points.

Figure 11 shows the time evolution up to the touch down of the water surface

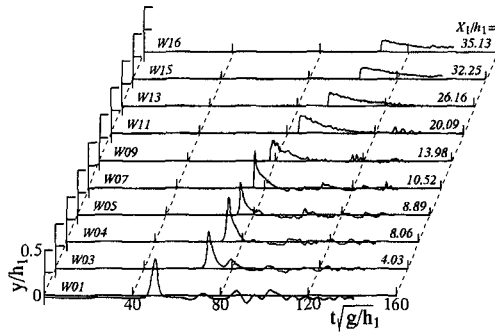
profiles of a composite breaker captured with the high speed video camera. The surface profile demonstrates that a remarkably large jet is formed by the composite breaker and is ejected from the 2nd crest developed by the coupling with the incident crest.

Figure 12 shows spatial changes of water surface elevations at measuring points from W01 to W16 of composite breakers with  $H_1/h_1 = 0.30, 0.42$  and  $0.55$  on a double reef with  $R_1/h_1 = 0.85, R_2/h_1 = 0.43$  and  $X_1/h_1 = 8.06$ . Each incident wave begins to break near the measuring point of W07. After that, the overturning jet from the 2nd crest touches down on the front face as shown in Fig.11, and further a bore front accompanying strong energy dissipation is formed.



(a)  $H_1/h_1 = 0.30$

(b)  $H_1/h_1 = 0.42$



(c)  $H_1/h_1 = 0.55$

Figure 12: Temporal water surface elevations at representative measuring points of the composite breaker

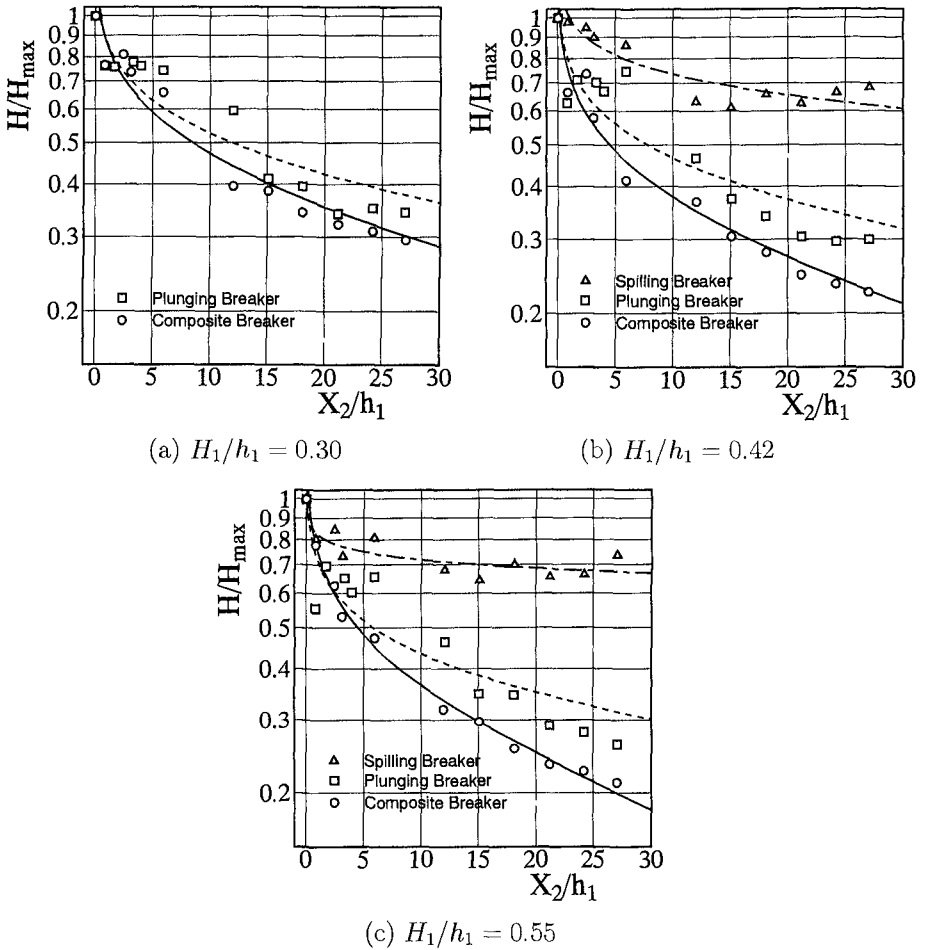


Figure 13: Wave height decay after breaking of the composite breaker

As a result, wave absorption is pronounced and the breaking wave propagates as bore-like wave while keeping a similar profile.

Figure 13 shows spatial variations of the wave height ratio  $H/H_{max}$  of the composite breakers on a double reef shown in Fig.12, together with those of a spilling breaker on a single reef of  $R/h_1 = 0.43$  and a plunging breaker on a single reef of  $R/h_1 = 0.85$ . The value of  $H/H_{max}$  strongly depends on breaker type ; the wave height of the composite breaker remarkably decays with the propagation distance after breaking, while those of the spilling breaker and the plunging one reach nearly stable state at  $X_2/h_1 \approx 10$  and  $20$  respectively.

Figure 14 shows the relations of the transmission coefficient  $K_T$  and reflec-

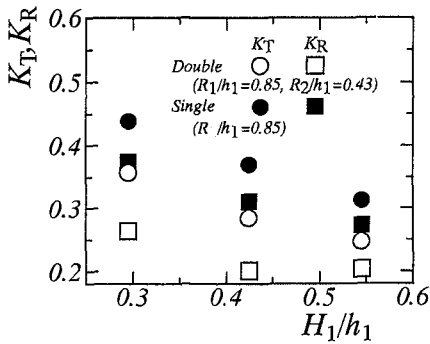


Figure 14: Comparisons of the transmission coefficient  $K_T$  and reflection one  $K_R$  between the composite breaker and plunging one under the same incident wave height  $H_1/h_1$

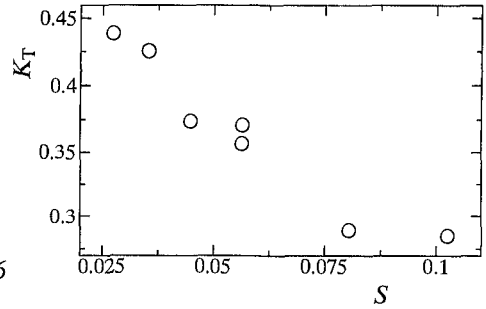


Figure 15: Relationships between the transmission coefficient  $K_T$  and the relative jet size  $S$

tion coefficient  $K_R$  to the incident wave height ratio  $H_1/h_1$ . The incident waves break on a double reef as a composite breaker, while they break on a single reef as a plunging breaker. Even if the incident wave is identical and further the crown height  $R_1$  of the double reef is the same with the crown height  $R_1$  of the single reef, both the coefficients  $K_R$  and  $K_T$  for waves incident to a double reef largely decrease in comparison with those for waves incident to a single reef, respectively by the depth change due to two steps and the generation of the composite breaker on the reef. Thus, by remodelling a single reef with  $R_1/h_1 = 0.85$  to a double reef with  $R_1/h_1 = 0.85$ ,  $R_2/h_1 = 0.43$  and  $X_1/h_1 = 8.06$ , it becomes possible to reduce both the values of  $K_T$  and  $K_R$  by more than 23% against the incident waves with  $H_1/h_1 = 0.30 \sim 0.55$ .

Figure 15 shows the relationships of the transmission coefficient  $K_T$  to the jet size  $S$  of various type breakers on single and double reefs. It is clearly found that the value of  $K_T$  decreases proportionally to the increase of the jet size and wave height decay after breaking is governed by the jet size itself. This result shows that the generation of the breaker forming a jet with larger size, that is, the generation of the composite breaker is efficient to the improvement of wave absorption.

## 6. Conclusions

A new type breaker forming a giant jet, referred here to as a composite breaker, is generated by the composition of fast growing 2nd crest and near-breaking incident crest suffering the reciprocal effect; the decaying effect due to the crest exchange with the 2nd crest generated by the 2nd step of a double reef and the shoaling effect due to the 2nd step. The reciprocal effect forms the strongly held triangular crown and produces a giant jet by incorporating the triangular crown into the 2nd crest. Such a breaker has not ever been known and are supposed to excite strong turbulence by its diving and cause the resultant remarkable dissipation. Therefore, development of a new wave control system utilizing a composite breaker could be expected.

### References

- Cooker, M.J., D.H. Peregrine, C. Vidal and J.W. Dold (1990): The interaction between a solitary wave and a submerged semicircular cylinder, *J. Fluid Mech.*, 125, 51-55.
- Galvin, C.L. (1968): Breaker type classification on these laboratory beaches, *J. Geophys. Res.*, 73/12, 3651-3659.
- Tanaka, M. (1986): The stability of solitary waves, *Physics of Fluids*, 29, 650-655.
- Yasuda, T., H. Hara and M. Tanaka (1990): A computational model of the deformation including overturning of a solitary wave over a submerged obstacle, *Proc. 3rd Int. Sympo. Fluid Dynamics, Nagoya, Japan*, 919-924.
- Yasuda, T., Y. Sakakibara and M. Hara (1992): BIM simulation on deformation up to breaking of solitary waves over uneven bottoms, *Proc. HY-DROSOFT92, Valencia, Spain*, 523-535.